Theoretical Model of Nonequilibrium Cluster Binding Energy to Optimize Chemical Properties

Shuai Zhang[a], Lei Chen[b,*], Wanli Zhu[c], Ruixin An[d]

[a]College of Materials Science and Engineering, Jilin Jian Zhu University, Changchun 130118, China
[b]College of municipal and environmental engineering, Jilin Jian Zhu University, Changchun 130118, China
[c]School of Geomatics and Prospecting Engineering, Jilin Jian Zhu University, Changchun 130118, China
[d]School of Transportation Science and Engineering, Jilin Jian Zhu University, Changchun 130118, China
chenlei@jlju.edu.cn

This paper builds three models about the surface volume ratio $\square$, the bonds ratio Ba / Bt and the binding energy Ec (N) of the Wulff construction with the total number of atoms, N, in the system as a variable. The results from model prediction are consistent with those from the appropriate cluster experiment and the computer simulation. In allusion to the uncertainty of the structure of atomic clusters, the geometric and energy models of Wulff structure are used to approximate the energy and morphology of clusters and optimize their chemical properties.

1. Introduction

It is well-known that the Wulff construction (available by taking the minimum surface energy per unit volume) is a standard method to get an equilibrium structure of bulk crystals. Although the atomic cluster differs from the Wulff construction, it has the lowest system surface energy just as crystals have. At this point, the cluster morphology and energy may be similar to Wulff construction (Zhu et al., 2011; Li et al., 2009; Li et al., 2013; Jiang et al., 2000).

The thermodynamic behavior of nanocrystals differs from that of their corresponding bulk materials mainly because of the large surface-to-volume ratio that strongly influences the chemical and physical properties of the nanocrystals. The broken bonds of surface atoms inevitably lead to the instability of materials at the nanoscale (e.g., decreased melting point and cohesive energy of ultrafine metallic particles with decreased size). Thus, a number of excellent models for size and shape dependence of the melting behavior of a nanosolid have been developed in terms of classical thermodynamics and modern molecular dynamics. In these models, the most important consideration is the surface-to-volume ratio because the vibration frequency of surface atoms is distinct from that of the inner ones. An exponential or linear relationship between the material size and thermodynamic function has been obtained, and the good reasonability of the established models has been proven. However, the bond characteristics of a system are unclear. In fact, the bond state of a system is directly related to the thermal properties. The atomic cohesive energy can be obtained from the average coordination number and bond strength per atom (Zhang and Chen, 2018).

Metallic nanomaterials have been the object of a growing interest due to their interesting properties (e.g. their electronic, magnetic, optic, catalytic, mechanical and thermodynamic properties) and have been widely used as functional materials in physics, chemistry, and biology. For practical application of nanomaterials, we need to know which structures are stable and whether they maintain their specific structures under given conditions. The most significant structural change originates from a solid-to-liquid phase transformation, namely, reasonable information on the solid-to-liquid transition is necessary. Therefore, with the miniaturization of devices, one has to envisage an insurmountable stability problem and understanding their thermodynamic properties is essential both for practical applications and from a fundamental point of view. As we all know, the melting temperature Tm is an important physical quantity accounting for the thermodynamics of materials, by which we can derive almost all thermodynamic properties of materials. And on the other hand, the properties of materials are functions of the ratio of working temperature to melting temperature. For nanomaterials, the

melting temperature have a decreasing tendency with the reduction of size which will increase the ratio and elevate the properties of nanomaterials. However, nanocatalysts might melt at temperatures far below the melting temperature of bulks and lose their predominant catalytic functionality. Therefore, melting becomes one of the failure modes at elevated temperatures for nanocatalysts. To resolve this limit, nanoscaled bimetallic alloys have been of special interest because of higher stability. Nanoscaled bimetallic alloys are a class of materials that show a combination of properties which are associated with the two constituent metals. In many cases, there is a great enhancement in their specific physical and chemical properties owing to a synergistic effect.

2. Model

As is known, nanoparticles are a state of matter that has properties different from either molecules or bulk solids, and thus their shape and structure of nanoparticles are strongly functions of the number of atoms (N) in a system. However, a nanoparticle with certain size usually has similar spherical shape in order to minimize surface energy although they could be in different structures, since surface energy directly determine the stability of different shapes and sizes, especially for the particles from 1nm to 100nm. Moreover, with size dropping, nanoparticles usually take the densest packing structure, for example, Na and Mo nanoparticles would have an FCC or more like icosahedron structures and Co nanoparticles with 4 N 60 have an icosahedron structure, while the structure becomes unstable for a large number of atoms and transforms into a Wulff construction, which is just a patch of the FCC lattice.

In view of the closed-packed arrangement of atomic clusters, a Wulff sphere construction of face-centered cubic crystal is referenced in this paper. The Wulff sphere is available by symmetrically shearing the six vertices of the octahedron, thereby (100) faces of six squares and (111) faces of eight hexagons are formed on surface. The Wulff sphere is just a chamfered octahedron TO structure. As shown in Fig. 1, for the (111) faces, there are three edges common to the (100) faces of the squares, on each of which the number of atoms is supposed to be n_{squ}. The number of atoms on the other three edges is supposed to be n_{hex}. As the number of bonds depends on the dimension and structure of the system simultaneously, in this paper, the geometric characteristics of the Wulff sphere construction are described with bonds ratio Ba / Bt as the variable, then,

$$\delta = N_s/N \tag{1}$$

Where N_s represents the number of atoms on the surface of the system. For the Wulff sphere construction, the surface atoms cover the atom $N_{(111)}$ on the (111) faces, the atom $N_{(100)}$ on the (100) faces, the atom N_e on the edge and the atom N_v on the vertex. Here, the ratio of surface to volume is used as mentioned in Jiang's work. Since is the simplest function to describe the shape effect of nanopaticles, the smaller the value, the more spherical the shape, and thus the smaller surface energy. It is clear that the same value for both Wulff construction and icosahedron is found and this is the smallest value compared with other shapes. Thus, taking Wulff shape to describe small nanoparticles becomes in valid within the acceptable error range. As size increases, 0 for any shape, that is to say the shape effect will disappear for larger particles. In addition, it is commonly observed that most of fcc particles correspond to the Wulff shape, and even can be extended to most closely packed materials, which is confirmed in other works where the most appropriate structure of the nanoparticles can also be Wulff. Based on the discussion above, taking Wulff structure as the shape of nanoparticles in this work is reasonable.

According to the Wulff sphere geometrical characteristics given in Fig. 1, $N_{(111)}$, $N_{(100)}$, N_e and N_v are expressed as follows:

$$N_{(111)} = 4[(n_{squ}+n_{hex})(n_{squ}+n_{hex}-9)+2n_{squ}n_{hex}+14] \tag{2}$$

$$N_{(100)} = 6(n_{squ}-2)^2 \tag{3}$$

$$N_e = 12(2n_{squ}+n_{hex}-6) \text{ and } N_v = 24 \tag{4}$$
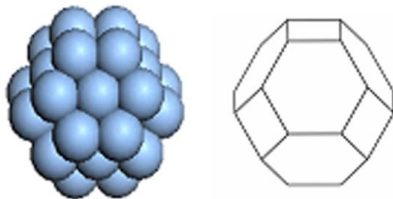

Figure 1: A sketch of a general TO structure with eight hexagonal (111) and six square (100) facets at surfaces (Gu et al., 2001; Coyle et al., 2001)

By adding the above formulae, the number of atoms on the surface of the system can be available, namely: N_s = $N_{111}+N_{100}+N_e+N_v$. Besides, as a function of n_{squ} and n_{hex}, the total number of atoms in the system, N, is determined by the following formula:

$$N=\{2[2(n_{squ}-1) + n_{hex}]^3+2(n_{squ}-1) + n_{hex}\}/3-2(n_{squ}-1)^3-3(n_{squ}-1)^2-(n_{squ}-1)$$ (5)

By defining the ligancy of the surface atoms in different positions and combining the number of corresponding surface atoms, the average ligancy Z_s of the surface atoms can be available,

$$Z_s=(Z_{(111)}N_{(111)}+Z_{(100)}N_{(100)}+Z_eN_e+Z_vN_v)/N_s$$ (6)

Where, $Z_{(111)}$, $Z_{(100)}$, Z_e and Z_v are the ligancies of the atoms on the (111) faces, on the (100) faces and at the vertices, then $Z_{111} = 9$, $Z_{100} = 8$, $Z_e = 7$, $Z_v = 6$. For face-centered cubic crystals, the ligancy of atoms in the bulk is 12, i.e. $Z_b = 12$. Therefore, the number of corresponding bonds is $B_a = [N_sZ_s+(N-N_s)Z_b]/2$ and $B_t = NZ_b/2$, that is:

$$\frac{B_a}{B_t} \quad \frac{N_sZ_s \quad (N \quad N_s)Z_b}{NZ_b}$$ (7)

It is difficult to determine arithmetic values δ and B_a/B_t for the Wulff sphere construction of different substances since there are two variables contained in the above formula, n_{squ} and n_{hex}. The two variables are therefore incorporated into one to simplify the calculation process, which can be achieved by considering the Wulff sphere construction formation conditions. For any Wulff sphere construction, the following conditions must be met:

$$\frac{\gamma_{(100)}}{\gamma_{(111)}} = \frac{D_{(100)}}{D_{(111)}}$$ (8)

Where $\gamma_{(100)}$ and $\gamma_{(111)}$ are the surface energies of (100) faces and (111) faces, respectively. D is the distance from the face to the center of the chamfered octahedron. It follows that the Wulff sphere construction depends on the substance itself, and its geometrical characteristics depend on the ratio $\gamma_{(100)}/\gamma_{(111)}$. In the formula (8), $D_{(100)}/D_{(111)}$ can be expressed as: $D_{(100)}/D_{(111)} = d_{(100)}(\xi_{(100)}-1)/d_{(111)}(\xi_{(111)}-1)$, where $d_{(100)}$ and $d_{(111)}$ are the interlayer spacings of the (100) faces and the (111) faces, respectively. For face-centered cubic crystal, $d_{(100)}/d_{(111)} = \sqrt{3}/2$. $\xi_{(100)}$ and $\xi_{(111)}$ are the number of layers of (100) faces and (111) faces at the intervals of $2D_{(100)}$ and $2D_{(111)}$, respectively. For a typical TO structure consisting of a hexagonal and a square facets, there is a relationship: $\frac{\xi_{100}}{\xi_{111}} = \frac{2n_{squ}+2n_{hex}-4}{2n_{squ}+2n_{hex}-3}$. According to the formula (8), this formula can be re-expressed as:

$$\frac{2\gamma_{(100)}}{\sqrt{3}\gamma_{(111)}} = \frac{2n_{squ} + 2n_{hex} - 4}{2n_{squ} + n_{hex} - 3}$$ (9)

The relationship between n_{hex} and n_{squ} can be determined from the formula (9) and based on the ratio $\gamma_{(100)}/\gamma_{(111)}$ for different substances. As shown in the Table 1, there are ratios of $\gamma_{(100)}/\gamma_{(111)}$ of the known face-centered cubic crystals. $\gamma_{(100)}$ is generally greater than $\gamma_{(111)}$ since the (100) face has more missing bonds, such that $\gamma_{(100)}/\gamma_{(111)} > 1$.

In the formula (9), n_{hex}/n_{squ} is a monotone function of $\gamma_{(100)}/\gamma_{(111)}$ and increases as the value of $\gamma_{(100)}/\gamma_{(111)}$ goes up. It means that the substance with a higher value $\gamma_{(100)}$ requires smaller (100) faces on its Wulff sphere construction surface. Note that, if $n_{hex} = n_{squ}$, $\gamma_{(100)}/\gamma_{(111)} = 2/\sqrt{3}$. This is a special Wulff sphere construction, also called as a regular chamfered octahedron (R-TO) whose surface is composed of regular hexagons and squares. It followed that, when $\gamma_{(100)}/\gamma_{(111)} > 2/\sqrt{3}$, $n_{hex} > n_{squ}$; when $\gamma_{(100)}/\gamma_{(111)} < 2/\sqrt{3}$, $n_{hex} < n_{squ}$. We note that there is a limit case, that is, for any value n_{hex}, $n_{squ} = 1$. This means the complete octahedral structure (OH) without any chamfer. However, OH structures are generally unstable due to their high energy status.

In order to compare with the real cluster structure, the geometric parameters of IH and CO structures are imported:

$$N_s=10(v-1)^2+2 \text{ (IH, CO)}$$ (10)

$$N = \frac{10}{3}v^3 - 5v^2 + \frac{11}{3}v - 1 \text{ (IH, CO)}$$ (11)

$$\frac{B_a}{B_t} = \frac{20v^3 - 45v^2 + 37v - 12}{20v^3 - 30v^2 + 22v - 6} \quad \text{(IH)} \tag{12}$$

$$\frac{B_a}{B_t} = \frac{10v^3 - 24v^2 + 20v - 6}{10v^3 - 15v^2 + 11v - 3} \quad \text{(CO)} \tag{13}$$

Where, since all the edges on the surfaces of the IH or CO structures are identical, v represents the number of atoms on each edge.

Due to the substitution of bonds which is directly correlated to the binding energy, based on the surface broken bond theory, the size-dependent binding energy function can be approximately expressed as follows:

$$E_c(N)/E_c(\infty) = [(B_a/B_t)^{1/2} + B_a/B_t]/2 \tag{14}$$

According to the formula (14), $E_c(N)$ is still in line with the broken bond theory, although the binding energy is proportional to B_a or $\sqrt{B_a}$. Thus the formula (14) can also be used to describe the binding energy of any system.

Table 1: The values of $\gamma_{(100)}$ and $\gamma_{(111)}$ and the corresponding ratios $\gamma_{(100)}/\gamma_{(111)}$ for FCC metallic elements. The presented $\gamma_{(100)}/\gamma_{(111)}$ values respectively for R-TO and OH structures are determined according to Wulff theorem (Eq. (8)) for comparison

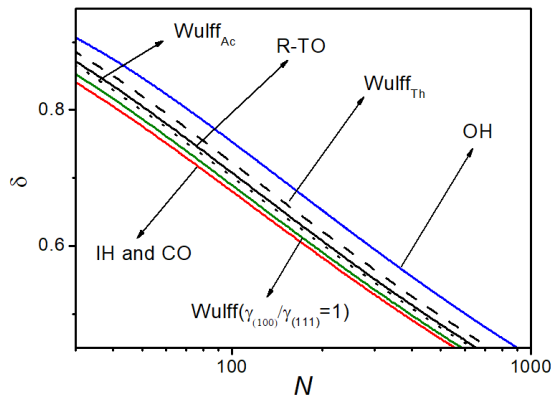| element	$\gamma_{(100)}$ (J m^{-2})	$\gamma_{(111)}$ (J m^{-2})	$\gamma_{(100)}/\gamma_{(111)}$
Au	1.80	1.52	1.184
Ag	1.40	1.20	1.167
Ni	2.88	2.44	1.180
Pd	2.15	1.85	1.162
Ca	0.5	0.43	1.163
Sr	0.39	0.33	1.182
Cu	2.17	1.83	1.186
Pt	2.98	2.54	1.173
Rh	3.15	2.7	1.167
Ir	3.74	3.19	1.172
Pb	0.64	0.55	1.164
Al	1.68	1.45	1.159
Ac	1.14	1.03	1.107
Th	2.36	1.85	1.276
R-TO			$2/\sqrt{3}=1.155$
OH			$\sqrt{3}=1.732$

3. Results and discussion

Figure 2: $\delta(N)$ functions for IH (and CO) and different Wulff constructions in terms of Eq. (3.1) (Biener et al., 2005; Volkert et al., 2006)

According to the formula (1), the surface volume ratios δ of IH, CO structures and Wulff sphere construction with different values of $\gamma_{(100)}/\gamma_{(111)}$ are subjected to change with the number of atoms N in the system, as shown in Fig. 2. δ is the simplest function used to describe the geometrical characteristics of clusters, where values δ of the IH and CO structures are equal. It is obvious from Fig. 2 that the error between IH (or CO) and the Wulff sphere construction is lower and tends to zero as the value N increases. The coincidence of function $\delta(N)$ of IH and Wulff sphere construction implies that the IH structure has a Wulff-like morphology. The relatively large δ error between IH and Wulff sphere construction suggests that even though the crystal structure takes the morphology of Wulff sphere, the number of atoms on its surface is still greater than the that on IH structure. Therefore, the morphology of clusters more tends to be spherical. On the other hand, when N is a constant, the value δ of Wulff sphere construction depends on the ratio of $\gamma_{(100)}/\gamma_{(111)}$. As shown in Fig. 2, as the value of $\gamma_{(100)}/\gamma_{(111)}$ decreases, the δ value falls down accordingly, which means that a higher value n_{squ} contributes to the formation of a spherical structure. This further explains that, compared with Wulff sphere construction,

CO structure has a lower value δ. Therefore, the minimum and maximum of the Wulff sphere construction correspond to $\gamma_{(100)}/\gamma_{(111)} = 1$ and $\gamma_{(100)}/\gamma_{(111)} = \sqrt{3}$, respectively, where $\gamma_{(100)}/\gamma_{(111)} = \sqrt{3}$ means OH structure. It is worth noting that in Fig. 2, the errors of the values δ of different Wulff sphere constructions are extremely lower, that is to say, the geometric error of the Wulff caused by different ratios of $\gamma_{(100)}/\gamma_{(111)}$ are negligible. Therefore, the standard Wulff sphere construction - R-TO ($\gamma_{(100)}/\gamma_{(111)} = 2/\sqrt{3}$) can approximately describe the function $\delta(N)$ of any atomic cluster within the error range.
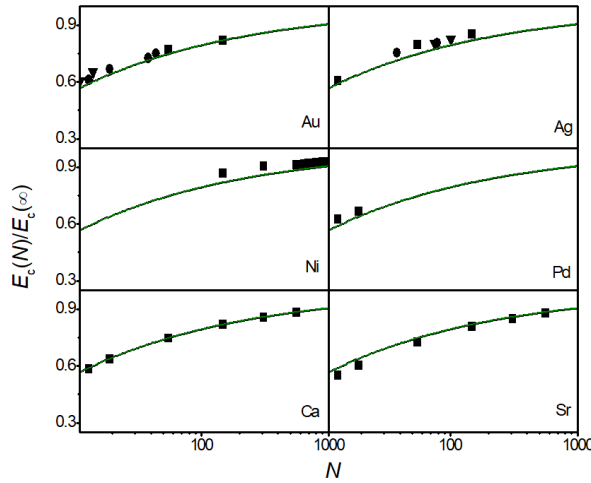

Figure 3: The comparison the function values Ba/Bt for different structures (Ouyang et al., 2006; Kofman et al., 1994; Jiang et al.,2001)

As shown in Fig. 3, the function values B_a/B_t for different structures are compared. It is found that the B_a/B_t is also correlated with structure and decreases as the number of atoms N falls down. The B_a/B_t of IH structure is greater than that of CO and Wulff in a full size range, which means that the total number of bonds in IH structure is highest. As shown in Fig. 3, it is also suggested that the B_a/B_t in CO structure is lower than that in any Wulff sphere construction, although it is also face-centered cubic crystal with the lowest value δ. Besides, a series of functions B_a/B_t for Wulff sphere construction with $\gamma_{(100)}/\gamma_{(111)}$ between 1 and √3 are given in Fig. 3. It is found that the B_a/B_t of OH structure is minimal, and the error in values B_a/B_t between different Wulff sphere structures is also negligible. Values B_a/B_t are correlated to the value δ on the one hand, or the surface morphology of the system and on the other hand have something to do with the binding energy $E_c(N)$. As a result, the Wulff sphere, the IH and the CO structures have similar values B_a/B_t, The Wulff construction can describe the characteristics of atomic clusters not only in morphology or structure, but also in binding energy.

4. Conclusion

Based on the total number N of atoms in the system, this paper gives three models for the surface volume ratio δ, the bonds ratio B_a/B_t and the binding energy $E_c(N)$ of the Wulff construction. The model prediction results are consistent with those of the corresponding atom cluster experiments and computer simulation. As a

consequence, even if the atomic cluster structure is uncertain, the geometry and energy model of the Wulff construction can be used to approximately describe the energy and morphology of the cluster.

Acknowledgment

References

Biener J., Hodge A.M., Hamza A.V., Hsiung L.M., Satcher J.H., 2005, Nanoporous Au: A high yield strength material, Journal of Applied Physics, 97, 024301-024305

Coyle S., Netti M.C., Baumberg J.J., Ghanem M.A., Birkin I.R., Bartlett D.M., Whittaker D.M., 2001, Confined Plasmons in Metallic Nanocavities, Physical Review Letters, 87, 176801-176805.

Gu L., Cheley S., Bayley H., 2001, Capture of a Single Molecule in a Nanocavity, Science, 291, 636-639.

Jiang Q., Zhang Z., Li J.C., 2000, Melting thermodynamics of nanocrystals embedded in a matrix, Acta Mater, 48, 4791-4795

Jiang Q., Liang L.H., Zhao D.S., 2001, Lattice Contraction and Surface Stress of fcc Nanocrystals, Journal of Physical Chemistry B, 105, 6275-6279.

Kofman R., Cheyssac P., Aouaj A., Lereah Y., Deutsche G., 1994, Surface melting enhanced by curvature effects, Surface Science, 303, 231-236.

Li H., Han P.D., Zhang X.B., Li M., 2013, Size-dependent melting point of nanoparticles based on bond number calculation, Materials Chemistry & Physics, 137, 1007-1011.

Li H., Zhao M., Jiang Q., 2009, Cohesive Energy of Clusters Referenced by Wulff Construction, Journal of Physical Chemistry C, 113, 7594-7597.

Ouyang G., Tan X., Cai M.O., Yang G.W., 2006, Surface energy and shrinkage of a nanocavity, Applied Physics Letters, 89, 183104-183109.

Volkert C.A., Lilleodden E.T., Kramer D., Weissmuller J., 2006, Approaching the theoretical strength in nanoporous Au, Applied Physics Letters, 89, 061920-061925

Zhang S., Chen L., 2018, Mechanism and application of photocatalytic hydrogen generation by cobalt oximes, Chemical Engineering Transactions, 64, 619-624. DOI: 10.3303/CET1864104

Zhu Y.F., Zheng W.T., Jiang Q., 2011, Distinct Young's modulus of nanostructured materials in comparison with nanocrystals, Physical Chemistry Chemical Physics Pccp, 13, 21328-21332.